TRIPLET CONFINEMENT INDUCED HIGH EFFICIENCY IN SINGLE LAYER DOPING OF PHOSPHORESCENT ORGANIC LIGHT-EMITTING DIODE

Agus Putu Abiyasa[1],I Wayan Sukadana[2], I Wayan Sutama[3], I Wayan Sugarayasa[4],Yoga Divayana[5]

[1, 2, 3, 4]Faculty of Engineering and Informatics, Undiknas University, Bedugul Street No 39, Denpasar, Indonesia
[5]Faculty of Engineering, Udayana University, Kampus Bukit Jimbaran, Badung, Indonesia
abiyasa@undiknas.ac.id[1]

ABSTRACT

In this research, we fabricated green phosphorescent organic light-emitting diodes with high quantum efficiency. A layer of sparsely distributed *fac* tris(2-phenyl-pyridinato-N,$C^{2'}$) iridium ($Ir(ppy)_3$) molecules was deposited between 4,4',4''-tris(N-carbazolyl) triphenylamine (TCTA) and 2,2',2''-(1,3,5-benzinetriyl)-tris(1-phenyl-1-h-benzimidazole) (TPBi) in the device. The measurement on triplet exciton distribution showed that the triplet exciton was highly confined at the TCTA/TPBi interface. By controlling the deposition rate and time, the effect of self–quenching of $Ir(ppy)_3$ molecules can be reduced that contribute to high eficiency light emission. The best device in our experiment has reached current efficiency of 52 cd/A, external quantum efficiency of 16 % and power efficiency of 52 lm/W.

Keywords: organic light emitting diodes;phosphorescence; brightness; polymers.

A. INTRODUCTION

Organic light-emitting diodes (OLEDs) have been regarded as one of the next generation display and lighting technologies because of their potential to achieve highly efficient devices at low cost and on flexible substrates (Tang et al, 1987), (Forrest, 2003) and (So et al, 2008). Phosphorescent organic light-emitting diodes (PHOLEDs) have attracted significant attention due to their capability of reaching 100% internal quantum efficiency (IQE) (Baldo et al, 1998). To achieve high efficiency PHOLEDs, co–evaporation of dopant and host materials is a common method used for the emitter layer deposition (Tang et al, 1989), also in previously proposed simplified architectures (Kim et al, 2009) and (Liu et al, 2009). On the other hand, there are also reports on the fabrication of the emitter layer without co–evaporation, e.g., using layer-by-layer deposition of host – dopant (Divayana et al, 2009). Another promising approach relies on the use of a single layer of ultra–thin dopant where the performance of the OLEDs has been shown to be comparable to those based on the co–evaporation technique.

Among these, the high efficiency of the devices in ultra–thin dopant architecturehas not been well understood yet. It has been suggested that the efficiency enhancement can be mainly due to high exciton confinement as well as efficient energy transfer that take place at the exciton formation zone. High exciton confinement can be achieved using high triplet-energy (E_T) material. A recent study on 4,4',4''-tris(N-carbazolyl) triphenylamine (TCTA) (E_T = 2.8 eV) as hole transport layer (HTL) has improved exciton confinement in EML compared to N,N'-bis(naphthalen-1-yl)-N,N'-bis(phenyl)-benzidine (NPB) (E_T = 2.3 eV). In addition, energy transfer from host to dopant is known to be highly efficient in co–evaporation doping system. When the dopant site is within the exciton diffusion length, host exciton will transfer its energy to the dopant and emit light efficiently. Doping concentration is typically <10% in *fac* tris(2-phenyl-pyridinato-N,$C^{2'}$) iridium:4,4'-N,N'-dicarbazole-biphenyl ($Ir(ppy)_3$:CBP) based emitter for the optimum concentration. For ultra–thin doping, sub–monolayer thickness (<1 nm) of dopant is used for high efficiency emitter (Zhao et al, 2013). It is possible that the sub–monolayer thickness in ultra–thin layer is analogous to optimal concentration in co–evaporation. Nevertheless, the importance and reason of sub–monolayer dopant thickness in ultra–thin doping have still not been understood.

In this work, to address these, we show that exciton confinement, efficient energy transfer and absent of concentration quenching at the vicinity of exciton formation zone contribute to the high efficiency in green phosphorescent OLEDs employing ultra–thin $Ir(ppy)_3$ dyes sandwiched between TCTA and 2,2',2''-(1,3,5-benzinetriyl)-

tris(1-phenyl-1-h-benzimidazole) (TPBi). TCTA and TPBi strongly confined triplet excitons and coupled with efficient energy transfer produced high electroluminescence in phosphorescent OLEDs. Furthermore, controlling the $Ir(ppy)_3$ deposition time at very slow rate minimizes concentration quenching. The optimum thickness of $Ir(ppy)_3$ was found to be 0.1 nm. The performance of our best device has achieved current efficiency (CE) of 52 cd/A, external quantum efficiency (EQE) of 16 % and power efficiency (PE) of 52 lm/W.

B. LITERATURE STUDY

The physical process of light emission in OLEDs is due to energy transfer of electrons from host materials to guest materials (Kappaun et al, 2008). There are three main mechanisms of these processes namely 1) long range Forster transfer, 2) short range Dexter transfer and 3) direct generation at guest materials. These mechanisms can be explained from the following Figure 1.

In Forster transfer, a significant overlap between emission spectrum of host materialwith the absorption spectrum of guest material is very important for efficient energy transfer.

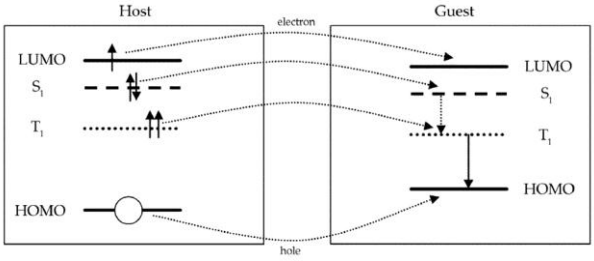

Figure 1 Energy transfermechanisms diagrams from host to guest materials in phosphorescent OLEDs (Source: Kappaun et al, 2008).

On the other hand, Dexter transfer requires the singlet and triplet excitons energy in host material to match the exciton energy in guest material. For direct generation, significant energy offset for HOMO and LUMO for the host and guest materials and carrier trapping at the guest materials will increase the light emission.

C. METHODOLOGY

The experiment was done by fabicrating the following devices. Device I consisting of glass/ITO(130 nm)/PEDOT:PSS(50 nm)/NPB(30 nm)/CBP(20nm)/$Ir(ppy)_3$(0.1nm)/TPBi(35 nm)/LiF(1 nm)/Al(150 nm) and Device II consisting of glass/ITO(130 nm)/PEDOT:PSS(50 nm)/NPB(30 nm)/TCTA(20 nm)/$Ir(ppy)_3$(0.1 nm)/TPBi(35 nm)/LiF(1 nm)/Al(150 nm).
ITO is a transparent electrode serving as the anode. PEDOT:PSS is the hole injection layer. NPB is the hole transporting layer. CBP or TCTA is the underlying host layer. TPBi is the electron transporting layer. LiF is the electron injection layer. Al is the cathode.

The details of device fabrication and measurement can be found from (Zhao et al, 2013) and (Liu et al, 2012). For the $Ir(ppy)_3$ deposition, the rate was set very low at 0.01 Å/s.

D. RESULTS AND DISCUSSION

In Figure 2, the schematic of energy band diagrams for Devices I and II are presented. The LUMO and HOMO level of the materials were taken from literature (Wang et al, 2011), (Hsiao et al, 2010) and (Jeon et al, 2008). In Figure 3, the current–voltage (J–V) and luminance–voltage (L–V) characteristics are shown. Devices I and II have similar thickness and hence their J–V characteristics depend on the energy barrier and mobility for the electron and hole transport. It is noted that CBP and TCTA have similar hole mobility values around $10^{-4}cm^2/V/s$. However, CBP has a much higher electron mobility ($\sim10^{-4}$ $cm^2/V/s$) compared to TCTA ($\sim10^{-8}$ $cm^2/V/s$). Therefore, CBP transports electron and hole equally (ambipolar) while TCTA is more of a hole transporter.

The J–V characteristics in Figure 3show that Devices I and II exhibit more or less similar behaviour. On the other hand, the L–V characteristics of Devices I and II are different where Device II has a much higher luminance level compared to Device I. This implies that the electroluminescence process is much better in Device II. A luminance level of > 10,000 cd/m^2 is achieved in Device II at an operational voltage of 6 V showing high performance of this device.

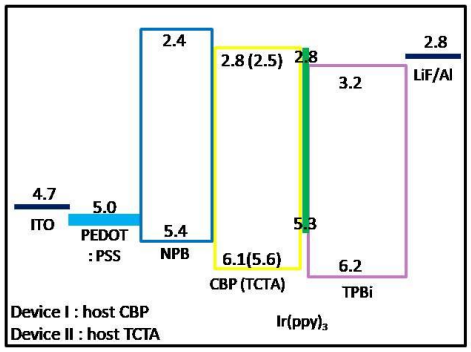

Figure 2 Schematic of energy bands diagrams of materials used in the device
(Source: author).

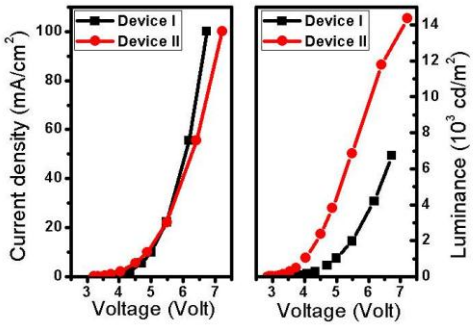

Figure 3 Current–voltage characteristics at 0.1, 1.0, and 10.0 mA/cm^2 of Devices I and II.
(Source: author).

In Figure 4, the EQE of both devices were measured from 0.1 to 100 mA/cm^2. At 0.1 mA/cm^2, Device I EQE is 2.5% and Device II EQE is 15%. At 1.0 mA/cm^2, Device I shows EQE of 4.9% while Device II shows 14.5%. At 10.0 mA/cm^2, Device I EQE drops to 3.8% while Device II drops to 11.3%.Interestingly, Device I exhibits EQE behaviour quite differently from Device II when operated from low to high current density. The EQE roll-off in Device II is slightly worse than that of Device I.

Overall, Device II shows over 3 times better EQE than Device I.As shown from Figure 3, the much higher measured EQE in Device II is due to better electroluminescence process contributed by theTCTA compared to CBP as the underlying layer for Ir(ppy)$_3$ dyes.

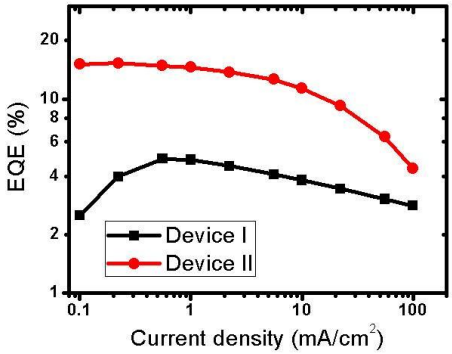

Figure 4 Measured External Quantum Efficiency (EQE) at 0.1, 1.0, and 10.0 mA/cm^2 of Devices I and II.
(Source: author).

To further understand this behaviour, the normalized spectra characteristics of Devices I and II are depicted in Figure 5. Besides the peak emission at 512 nm from Ir(ppy)$_3$, Device I has additional emission centered at 430 nm, which increases with the increasing current injection relative to the peak at 512 nm. We can relate the peak emission at 430 nm to NPB emission. At 0.1 mA/cm^2, NPB emission observed is very minimum. Since electrons and holes will mainly recombine near CBP/TPBi interface, Ir(ppy)$_3$ will efficiently capture the excitons. Due to ambipolar of CBP, more electrons will be able to transport into CBP and form excitons close to NPB when the current injection increases. Hence, NPB emission increases significantly.

On the other hand, Device II emission peaks at 512 nm due to Ir(ppy)$_3$ emission and the NPB emission is not observed with the increasing current injection. TCTA with a high triplet energy of 2.8 eV, much higher than Ir(ppy)$_3$ triplet energy of 2.4 eV, will block the triplet excitons diffusion to NPB. Therefore, much more triplet excitons contribute to energy transfer into Ir(ppy)$_3$ for light emission.

TCTA shows outstanding behaviour as the underlying material for Ir(ppy)$_3$ layer in ultra–thin single layer doping phosphorescent OLEDs. Due to its high triplet energy and low electron mobility,

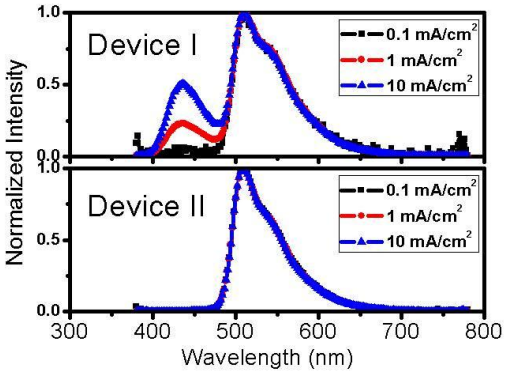

Figure 5 Normalized spectral characteristics at 0.1, 1.0, and 10.0 mA/cm^2 of Devices I and II. (Source: author).

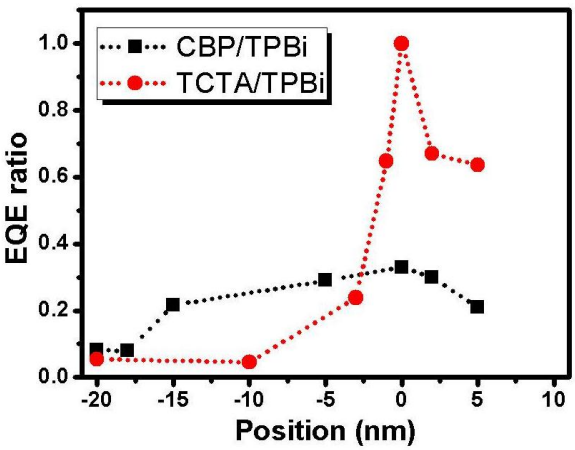

Figure 6 Triplet excitons distribution in Device I(II) as measured using Ir(ppy)$_3$ as sensor across the CBP(TCTA) and TPBi layers. The EQE ratio is normalized to the highest EQE measured from Device II. (Source: author).

the exciton formation at TCTA/TPBi interface will be more efficient than CBP/TPBi interface and at the same time confines the triplet excitons strongly at the interface. We further investigate on the triplet excitons distribution inside Devices I and II using the method that has been reported (Sun etal, 2006). We fabricate a similar device structure as in Device I (II) but with the ultra–thin layer of Ir(ppy)$_3$ is moved across the CBP (TCTA) to act as triplet exciton sensor. The thickness of Ir(ppy)$_3$ is kept the same for all device configurations.

We then measured the EQE of each device and plotted the result in Figure 6. All the EQE values have been normalized to the highest efficiency measured, which is from Device II structure.

Figure 6 presents the EQE ratio to the highest measured EQE as a function of Ir(ppy)$_3$ position in Devices I and II. The origin is defined at the CBP(TCTA)/TPBi interface for Device I(II) as depicted in the schematic diagram in Figure 2.

From Figure 6, the highest measured EQE is obtained when Ir(ppy)$_3$ located at the origin of Device II structure. The highest EQE of Device I reaches only 0.3 times compared to that of Device II. When Ir(ppy)$_3$ sensor is moved toward NPB, EQE of Device I drops slowly until it is very near to NPB where the EQE becomes significantly low. At Ir(ppy)$_3$ position very close to NPB < 5 nm, the triplet is effectively quenched by NPB in Device I. The relatively flat roll-off of EQE with respect to the position of Ir(ppy)$_3$ across the CBP layer implies that concentration of triplet excitons is almost uniform in CBP layer.

Device II, however, shows very different EQE behaviour when Ir(ppy)$_3$ is positioned away from the origin toward NPB. As the maximum EQE is observed at the origin, the value has been reduced to almost half even only when Ir(ppy)$_3$ is positioned 3 nm away from the origin. The value decays exponentially and becomes significantly small near NPB. This implies that triplet excitons must be highly confined at the TCTA/TPBi interface. In Figure 6, the triplet excitons also diffuse toward the TPBi layer. TPBi triplet energy (E_T = 2.7 eV) is less compared to TCTA and, hence, the confinement effect is not as strong as TCTA. However, the value has been reduced to almost half at a position >5 nm showing good triplet confinement behaviour. These suggest that TCTA and TPBi are suitable for triplet excitons confinement in ultra–thin dopant OLEDs architecture.

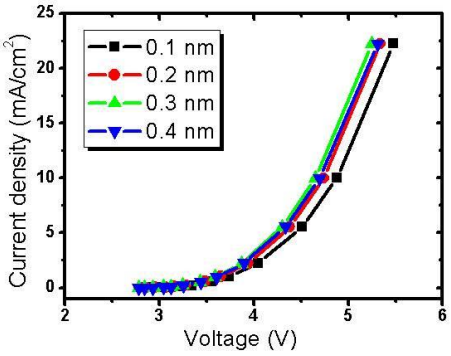

Figure 7 Current–voltagecharacteristics with increasing $Ir(ppy)_3$ thickness.
(Source: author).

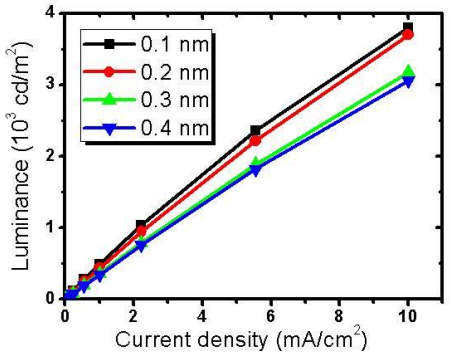

Figure 8 Luminance–voltagecharacteristics with increasing $Ir(ppy)_3$ thickness.
(Source: author).

Furthermore, the effect of varying thickness of $Ir(ppy)_3$ is also investigated for Device II. It has been reported that $Ir(ppy)_3$ will have low quantum yield in neat films due to concentration quenching (Zhang et al, 2010). In ultra–thin doping, sub–monolayer recorded thickness (below 1 nm) implies less dense $Ir(ppy)_3$ molecules. Therefore, it is thought that concentration quenching can also be minimized.

Next, the performance of OLED is shown as a function of the $Ir(ppy)_3$ thickness. Figure 7provides the J–V characteristics of such device. As expected all devices exhibit similar behaviour. This implies that the $Ir(ppy)_3$ layer does not affect the charge transport significantly. In Figure 8, the L–J characteristics of the devices are depicted. The

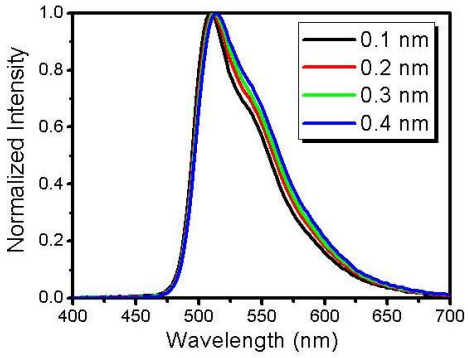

Figure 9 The normalized spectra at 0.01 $mA/cm^2$with increasing $Ir(ppy)_3$ thickness.
(Source: author).

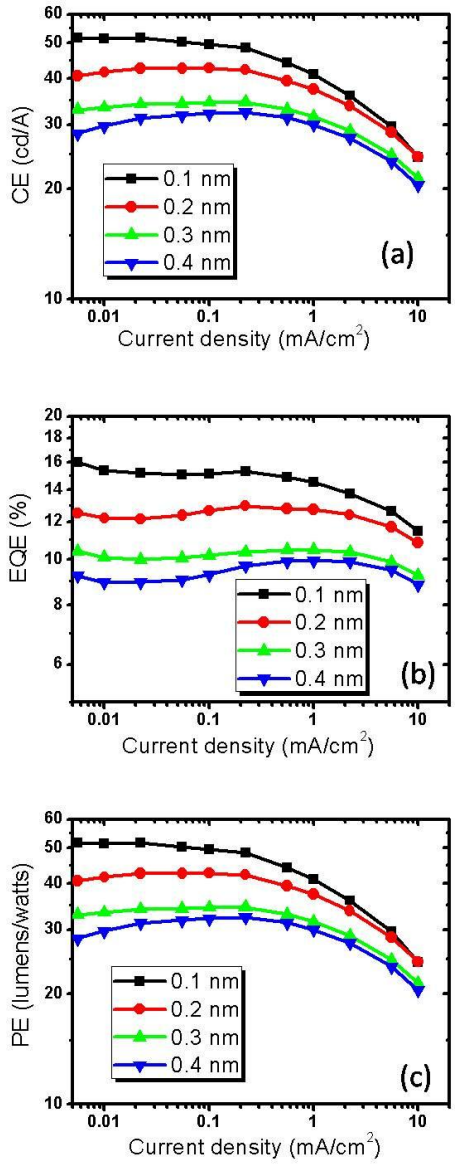

Figure 10(a) – (c) show CE, EQE, and PE, respectively, with the increasing $Ir(ppy)_3$ thickness as a function of the current density.
(Source: author).

luminance is the highest for 0.1 nm in wide range current density. The luminance isreduced when the thickness is increased from 0.1 to 0.4 nm.

In Figure 9, the normalized spectra are given for $Ir(ppy)_3$ thickness from 0.1 to 0.4 nm. The peak is observed at 512 nm with a shoulder at 546 nm. With increasing thickness from 0.1 to 0.4 nm, the peak shifts slightly from 512 to 514 nm. The shoulder at 546 nm shows increase in relative intensity with the increasing thickness.

In Figures 10(a)-(c), CE, EQE and PE of the devices are presented, respectively. The trend is similar where all performance levels drop with the increasing $Ir(ppy)_3$ thickness from 0.1 to 0.4 nm.
We relate the drop in the device performance to the concentration quenching when the $Ir(ppy)_3$ thickness is increased from 0.1 to 0.4 nm. As reported in literature, there are two possible ways of concentration quenching: molecule aggregation (Zhang et al, 2010) and long–range dipole quenching (Kawamura et al, 2006). The peak emission at 512 nm, which is due to $Ir(ppy)_3$ monomer emission, is quenched quite significantly. In molecule aggregation, adjacent $Ir(ppy)_3$ monomers will interact to form excimer states and additionally emit at longer wavelengths about 546 nm. With increasing aggregation, this shoulder emission at 546 nm will increase relatively to the peak emission at 512 nm. Based on Figure 9, the spectra changes fit the description of molecule aggregation condition. Therefore, we can conclude that the efficiency drop in our devices is mainly due to molecules aggregation effect.

E. CONCLUSION

In conclusion, we have investigated the mechanisms of high EQE phosphorescent OLEDs in ultra–thin dopant architecture. Here it has been shown that enhanced triplet excitons confinement at the vicinity of the exciton formation zone at TCTA/TPBi interface enabled host–guest energy transfer for efficient electroluminescence. Furthermore, it has also been demonstrated that $Ir(ppy)_3$ of 0.1 nm thickness is optimum to remove the concentration quenching. The best device has reached high CE, EQE, and PE of 52 Cd/A, 16%, and 52 lm/W, respectively.

ACKNOWLEDGEMENT

The authors would like to express his gratitude towards Luminous! Center of Excellence for Semiconductor Lighting and Displays at Nanyang Technological University Singapore that has given all the facilities support for the completion of this work.

REFERENCES

Baldo, M. A., O'brien, D. F., You, Y., & Shoustikov, A. (1998). Highly efficient phosphorescent emission from organic electroluminescent devices. *Nature*, *395*(6698), 151.

Divayana, Y., & Sun, X. W. (2009). An efficient bis (2-phenylquinoline)(acetylacetonate) iridium (III)-based red organic light-emitting diode with alternating guest: host emitting layers. *Organic Electronics*, *10*(2), 320-325.

Forrest, S. R. (2003). The road to high efficiency organic light emitting devices. *Organic Electronics*, *4*(2), 45-48.

Hsiao, C. H., Liu, S. W., Chen, C. T., & Lee, J. H. (2010). Emitting layer thickness dependence of color stability in phosphorescent organic light-emitting devices. *Organic Electronics*, *11*(9), 1500-1506.

Jeon, W. S., Park, T. J., Kim, S. Y., Pode, R., Jang, J., & Kwon, J. H. (2008). Low roll-off efficiency green phosphorescent organic light-emitting devices with simple double emissive layer structure. *Applied Physics Letters*, *93*(6), 293.

Kappaun, S., Slugovc, C., & List, E. J. (2008). Phosphorescent organic light-emitting devices: Working principle and iridium based emitter materials. *International journal of molecular sciences*, *9*(8), 1527-1547.

Kawamura, Y., Brooks, J., Brown, J. J., Sasabe, H., & Adachi, C. (2006). Intermolecular interaction and a concentration-quenching mechanism of phosphorescent Ir (III) complexes in a solid film. *Physical review letters*, *96*(1), 017404.

Kim, S. Y., Jeon, W. S., Park, T. J., Pode, R., Jang, J., & Kwon, J. H. (2009). Low voltage efficient simple p-i-n type electrophosphorescent green organic light-emitting devices. *Applied Physics Letters*, *94*(13), 98.

Liu, S. W., Divayana, Y., Abiyasa, A. P., Tan, S. T., Demir, H. V., & Sun, X. W. (2012). On the triplet distribution and its effect on an improved phosphorescent organic light-

emitting diode. *Applied Physics Letters*, *101*(9), 093301.

Liu, Z., Helander, M. G., Wang, Z., & Lu, Z. (2009). Efficient single layer RGB phosphorescent organic light-emitting diodes. *Organic Electronics*, *10*(6), 1146-1151.

So, F., Kido, J., & Burrows, P. (2008). Organic light-emitting devices for solid-state lighting. *Mrs Bulletin*, *33*(7), 663-669.

Sun, Y., Giebink, N. C., Kanno, H., Ma, B., Thompson, M. E., & Forrest, S. R. (2006). Management of singlet and triplet excitons for efficient white organic light-emitting devices. *Nature*, *440*(7086), 908.

Tang, C. W., & VanSlyke, S. A. (1987). Organic electroluminescent diodes. *Applied physics letters*, *51*(12), 913-915.

Tang, C. W., VanSlyke, S. A., & Chen, C. H. (1989). Electroluminescence of doped organic thin films. *Journal of Applied Physics*, *65*(9), 3610-3616.

Wang, Z. B., Helander, M. G., Qiu, J., Puzzo, D. P., Greiner, M. T., Liu, Z. W., & Lu, Z. H. (2011). Highly simplified phosphorescent organic light emitting diode with> 20% external quantum efficiency at> 10, 000 cd/m 2. *Applied Physics Letters*, *98*(7), 39.

Zhang, Y. Q., Zhong, G. Y., & Cao, X. A. (2010). Concentration quenching of electroluminescence in neat Ir (ppy) 3 organic light-emitting diodes. *Journal of Applied Physics*, *108*(8), 083107.

Zhao, Y., Chen, J., & Ma, D. (2013). Ultrathin nondoped emissive layers for efficient and simple monochrome and white organic light-emitting diodes. *ACS applied materials & interfaces*, *5*(3), 965-971.